Archives of Biochemistry and Biophysics 502 (2010) 23–30

Contents lists available at ScienceDirect

Archives of Biochemistry and Biophysics

journal homepage: www.elsevier.com/locate/yabbi

# Ribokinase family evolution and the role of conserved residues at the active site of the PfkB subfamily representative, Pfk-2 from *Escherichia coli*

Ricardo Cabrera, Jorge Babul, Victoria Guixé *

*Departamento de Biología, Facultad de Ciencias, Universidad de Chile, Casilla 653, Santiago, Chile*

ARTICLE INFO

*Article history:*
Received 7 May 2010
and in revised form 18 June 2010
Available online 25 June 2010

*Keywords:*
Ribokinase family
PfkB subfamily
Phosphofructokinase
Phosphoryl transfer mechanism

ABSTRACT

Phosphofructokinase-2 (Pfk-2) belongs to the ribokinase family and catalyzes the ATP-dependent phosphorylation of fructose-6-phosphate, showing allosteric inhibition by a second ATP molecule. Several structures have been deposited on the PDB for this family of enzymes. A structure-based multiple sequence alignment of a non-redundant set of these proteins was used to infer phylogenetic relationships between family members with different specificities and to dissect between globally conserved positions and those common to phosphosugar kinases. We propose that phosphosugar kinases appeared early in the evolution of the ribokinase family. Also, we identified two conserved sequence motifs: the TR motif, not described previously, present in phosphosugar kinases but not in other members of the ribokinase family, and the globally conserved GXGD motif. Site-directed mutagenesis of R90 and D256 present in these motifs, indicate that R90 participates in the binding of the phosphorylated substrate and that D256 is involved in the phosphoryl transfer mechanism.

© 2010 Elsevier Inc. All rights reserved.

## Introduction

The ATP-dependent phosphorylation of fructose-6-P or fructose-1-P to produce fructose-1,6 bisphosphate, and tagatose-6-phospahte to produce tagatose-1,6-bisphosphate, are important reactions in sugar catabolic pathways of bacteria. These enzymatic activities, namely 6-phosphofructokinases, 1-phosphofructokinases and 6-phosphotagatokinases, could be found within the ribokinase family of sugar kinases. The first two structures of phosphosugar kinases from the ribokinase family have been recently reported. Our group determined the crystal structure of the 6-phosphofructokinase isozyme 2 (Pfk-2, E.C. 2.7.1.11) from *Escherichia coli* in its tetrameric form in complex with two ATP molecules per monomer [1]. This enzyme is active as a dimer but is inhibited and form tetramers in the presence of high concentrations of the substrate MgATP [2]. This regulatory mechanism is modulated by the fructose-6-P concentration and has been demonstrated to be important for avoiding futile cycle occurrence under gluconeogenic conditions [3]. Previously, Miallau et al. (2007) reported the crystal structures of *Staphylococcus aureus* (*S. aureus*) tagatose-6-P kinase representing the apo, binary and ternary complexes of the enzyme with substrate and analogues, illustrating aspects of substrate recognition [4]. Interestingly, they identified a conserved motif, SGSLPXG, specific for phosphosugar kinases of the ribokinase family. However, up-to-date, no site-directed mutagenesis studies have been reported to evaluate the role of conserved residues at the active site of phosphosugar kinases from the ribokinase family.

Enzymes with a variety of specificities have been grouped within the ribokinase family. The evolutionary relatedness between Pfk-2 (from *E. coli*), tagatose-6-P kinase (LacC from *S. aureus*), 1-phosphofructokinases (from *E. coli* and *Rhodobacter capsulatus*) and ribokinase (from *E. coli*) was first recognized by Orchard and Kornberg in 1990 [5] and Wu et al. in 1991 [6]. Bork et al. (1993) identified sequence patterns common to phosphosugar kinases, ribokinases, fructokinases and inosine-guanosine kinases [7]. More recently, new members were further identified in the UniProtKB Swiss-Prot database (http://www.expasy.ch/prosite/) using the two highly conserved motifs assigned to the ribokinase family (accession numbers PS00583 and PS00584) [8].

After the crystal structure determination of *E. coli* ribokinase in 1998 by Sigrell et al. [9], structures of several other enzymes were documented to share the two-domain fold and characteristic topology of ribokinase. These enzymes are: the adenosine kinases from *Homo sapiens* [10] and *Toxoplasma gondii* [11,12], Aminoimidazole riboside kinase (AIR kinase)[1] from *Salmonella enterica* [13], 2-keto-3-deoxy gluconate kinase from *Thermus thermophilus* [14], nucleoside kinase from *Metanocaldococcus* [15], adenosine kinase from *Mycobacterium tuberculosis* [16], tagatose-6-P kinase from

* Corresponding author. Address: Laboratorio de Bioquímica y Biología Molecular, Departamento de Biología, Facultad de Ciencias, Universidad de Chile, Santiago, Casilla 653, Chile. Fax: +56 2 2712983.
*E-mail address:* vguixe@uchile.cl (V. Guixé).

[1] *Abbreviations used:* AIR kinase, aminoimidazole riboside kinase; Pfk-2, phosphofructokinase-2; SEC, Size-exclusion chromatography; PdxK, pyridoxal kinase

0003-9861/$ - see front matter © 2010 Elsevier Inc. All rights reserved.
doi:10.1016/j.abb.2010.06.024

*Staphylococcus aureus* [4], phosphofructokinase-2 from *E. coli* [1], the 2-keto-3-deoxy gluconate kinases from *Termothoga maritima* [17] and *Sulfolobus solfataricus* [18], and ketohexokinase from *Homo sapiens* [19]. Furthermore, several unpublished structures have been deposited in the PDB and classified as homologous to ribokinase at the SCOP [20] and CATH [21] databases. The tertiary structure in these enzymes consists of a major domain, with a central beta sheet with the arrangement 5↑4↑1↑8↑9↑10↑11↑12↓13↑ (in which strands 11 to 13 form a β-meander) surrounded by α-helices, and a minor domain containing a four stranded beta sheet with the arrangement 3↓2↑6↑7↓. The minor domain covers the active site as a lid and also contributes hydrogen bonding and Van der Waals interactions that result, for most of the members, in a dimeric association. These dimers can form higher oligomeric states (like tetramers, in the case of Pfk-2 in the presence of MgATP [1]) or hexamers, in the case of 2-keto-3-deoxygluconate kinase [14]). A monomeric state is observed in the case of eukaryotic adenosine kinases due to the insertion of complete secondary structure elements that occlude the interfacial surface [10].

How are evolutionarily related the phosphosugar kinases to the other members of the ribokinase family? The sequence identities of these proteins are in the range of 18–22% [15] making it difficult to clearly establish phylogenetic relationships by conventional multiple sequence alignment tools. The question on how the structural repertoire of ribokinase family members in the PDB may help to identify these relationships has not been explored in spite of the increasing availability of these structures.

All members of the ribokinase family phosphorylate sugars and sugar-derived compounds bearing a hydroxymethyl group. When the structures of the different protein–ligand complexes are superimposed, the sugar rings of AIRs, ribose and adenosine occupy the same location with their hydroxymethyl groups oriented in the same way [13], allowing a hydrogen bond interaction with a strictly conserved aspartic residue. This residue is conserved even at the superfamily level and it has been proposed previously that it acts as the catalytic base which deprotonizes the secondary hydroxyl group in the sugar substrate that will attack γ-phosphate of ATP [22]. The GAGD motif containing this aspartic is one of the sequence patterns originally identified in the studies by Bork et al. [7] that corresponds to the PS00584 motif in Prosite (see above). On the other hand, at the phosphosugar kinase subfamily level, conserved residues at the active site must account for the interaction with a common feature of these substrates, the phosphoryl group. For example, the serine residue described to interact with the phosphate of tagatose-6-P in *S. aureus* tagatose-6-P kinase is conserved in other phosphosugar kinases [4].

In this work, we perform a phylogenetic analysis to distinguish evolutionary relationships between ribokinase family members with known structure, which also allow us to recognized two kinds of sequence motifs; one conserved in the entire ribokinase family (GXGD) and a new motif (TR) exclusively conserved among the phosphosugar kinases. The role of these motifs was assessed by site-directed mutagenesis in Pfk-2 since it is the best characterized member among the phosphosugar kinases, biochemically and structurally speaking. Our results constitute, up to date, the most complete study of the role of conserved active site residues in substrate binding, catalysis and allosteric regulation for a phosphosugar kinase of the ribokinase family.

## Materials and methods

### *Dataset of ribokinase family members*

In the SCOP database the ribokinase-like family (SCOP id.: 53614) includes 9 different protein domains (domain is the unit of description and classification in these databases) from bacterial, eukaryal and archaeal species. In order to obtain a complete dataset, structures not present in these databases were exhaustively searched in the PDB (http://www.rcsb.org) with the "advanced search" tool, by performing a blast search using as the input query the sequences of every structure identified in SCOP. A total of 70 pdb files were found corresponding to different crystalline forms of 32 unique proteins. A non-redundant set of individual chains (Table 1) was generated by selecting for those structures with ligands present at the sugar binding site or closed orientations of their minor and major domains.

### *Structural alignment and phylogenetic analysis*

All proteins in our non-redundant dataset (Table 1) were structurally aligned by using the STAMP tool from Multiseq [23] in VMD [24]. The loops connecting β2–β3 and β6–β7 in the minor domain were removed since their structural differences drastically reduced the performance of superposition. The multiple sequences alignment (MSA) was obtained from the equivalent residues of the 32 superposed structures. Some misaligned positions were corrected by visual inspection. Finally, all the gap-including positions were removed using GeneDoc [25] giving as result a MSA of 188 positions × 32 taxa. The remaining positions correspond to the core of the ribokinase-like fold (Fig. 1B). Considering that Pfk-2 has 309 residues, these positions correspond to 61% of its entire length. We prepared our MSA in this way in order to work with Mr. Bayes v3.1.2 [26]. This program is not able to treat the insertion–deletion process under a realistic stochastic model. Since it treats gaps as missing data, gap-containing columns will not contribute with phylogenetic information. For the analysis, we use blosum62 as the fixed rate model and gamma-shaped rate variation across sites with a proportion of invariable sites. The number of generations was set to $4 \times 10^6$, obtaining for the average standard deviation of the split frequencies a value lower than 0.01.

### *Site-directed mutagenesis of Pfk-2*

Site-directed mutagenesis of D256 and R90 were carried out using the QuickChange (Stratagene) system using as the template the pET21d plasmid (Novagen) carrying the wild type *pfk-2* gene. The mutagenic primers were 5′-GAAGCCAAAGACTGGACC**AG**CA GAATTTACAC-3′ and 5′-ACCGTTGGCGCTGGT**AA**CAGCATGGTCGGC GCG-3′ for R90Q mutation and D256N mutation, respectively (mutated codon is underlined, the replaced nucleotide is in bold). The bases changed were verified by DNA sequencing of the mutants.

### *Enzyme expression and purification*

The mutant enzymes were produced in *E. coli* DF1020 since this strain does not express wild type phosphofructokinases. DF1020 strain was co-transformed with plasmid pGP1-2 [27] that allows the expression of the T7 RNA polymerase after heat induction and the pET21d plasmid carrying the Pfk-2 mutated gene. Cultures were grown at 30 °C in Luria broth media supplemented with ampicillin and kanamycin to a final concentration of 100 and 75 μg/ml, respectively. Protein expression was induced when the $A_{600}$ = 0.5 by heat treatment at 42 °C for 20 min; thereafter, the culture was incubated at 37 °C for 4 h before the cells were collected by centrifugation. The mutant enzymes were purified essentially as described in Babul [28], replacing the AMP-agarose step with a second chromatography in Cibacron blue-Sepharose. The transformed *E. coli* strains produced an average of 10–15 mg of protein per liter of culture. Protein concentration was determined using the Bio-Rad protein assay with the standard curve constructed with bovine serum albumin.

**Table 1**
Non-redundant set of structural representatives of the ribokinase family.

| PDBid* | Enzyme** | Organism | Ligand at the sugar site*** |
|---|---|---|---|
| 2nwh | Carbohydrate kinase | *Agrobacterium tumefaciens* | (Cl) |
| 3cqd | 6-Phosphofructokinase isozyme 2 | *Escherichia coli* | – |
| 2abq | Fructose 1-phosphate kinase | *Bacillus halodurans* | (Phosphate) |
| 2jg5 | Putative fructose 1-phosphate kinase | *Staphylococcus aureus* | – |
| 2ajr | Possible 1-phosphofructokinase | *Thermotoga maritima* | (Acetate) |
| 2f02 | Tagatose-6-phosphate kinase | *Enterococcus faecalis* | – |
| 2jg1 | Tagatose-6-phosphate kinase | *Staphylococcus aureus* | Tagatose-6-phosphate |
| 3ie7 | Phosphofructokinase, EC: 2.7.1.- | *Listeria innocua* | (Glycerol and Mg) |
| 3jul | Tagatose-6-phosphate kinase | *Listeria innocua* | Tagatose-6-phosphate |
| 1tz6 | Aminoimidazole riboside kinase (putative sugar kinase) | *Salmonella enterica* | Aminoimidazole riboside |
| 3iq0 | Putative ribokinase II (EC: 2.7.1.-) | *Escherichia coli* | – |
| 2qhp | Fructokinase | *Bacteroides theaiotaomicron* | – |
| 3gbu | Sugar kinase, EC: 2.7.1.- | *Pyrococcus horikoshii* | – |
| 2qcv | Putative 5-dehydro-2-deoxygluconate kinase | *Bacillus halodurans* | – |
| 1v1a | 2-Keto-3-deoxygluconate kinase | *Thermus thermophilus* | 2-Keto-3-deoxygluconate |
| 2afb | 2-Keto-3-deoxygluconate kinase | *Thermotoga maritima* | – |
| 2dcn | 2-Keto-3-deoxygluconate kinase, hypothetical fructokinase | *Sulfolobus tokodaii* | 2-Keto-6-phosphogluconate |
| 2var | 2-Keto-3-deoxygluconate kinase, fructokinase | *Sulfolobus solfataricus* | 2-Keto-3-deoxygluconate |
| 3in1 | Putative ribokinase, EC: 2.7.1.- | *Escherichia coli* | – |
| 1vm7 | Ribokinase | *Thermotoga maritima* | – |
| 2fv7 | Ribokinase | *Homo sapiens* | – |
| 1gqt | Ribokinase | *Escherichia coli* | Ribose |
| 3i3y | Ribokinase | *Klebsiella pneumoniae* | Ribose |
| 1vk4 | Carbohydrate kinase | *Thermotoga maritima* | – |
| 3kd6 | Nucleoside kinase | *Chlorobium tepidum* | Adenosine monophosphate |
| 2pkm | Adenosine kinase | *Mycobacterium tuberculosis* | Adenosine |
| 2c49 | Nucleoside kinase | *Methanocaldococcus jannaschii* | Adenosine |
| 3bf5 | Putative ribokinase | *Thermoplasma acidophilum* | – |
| 2hw1 | Ketohexokinase, fructokinase | *Homo sapiens* | Fructose |
| 2rbc | Putative ribokinase, EC: 2.7.1.- | *Agrobacterium tumefaciens* | (Glycerol) |
| 1lii | Adenosine kinase | *Toxoplasma gondii* | Adenosine |
| 1bx4 | Adenosine kinase | *Homo sapiens* | Adenosine |

* Order and grouping according to Fig. 1A.
** According to the TITLE and COMPND lines of the PDB file.
*** Indicated within parentheses when it is not the cognate substrate.

*Enzyme assays*

Phosphofructokinase activity was determined spectrophotometrically by coupling the fructose-1,6-bisphosphate production to the oxidation of NADH at pH 8.2 as described previously [29].

*Fluorescence Measurements*

All fluorescent titrations were performed using a Perkin–Elmer LS 50 fluorometer. Pfk-2 titrations and the subsequent fluorescence measurements were performed as previously described by Guixé et al. [30]. Briefly, Pfk-2 samples (1.6–2 μM) were incubated in 20 mM Hepes, pH 8.0, 5 mM DTT and 5 mM $MgCl_2$ and subsequent aliquots of fructose-6-P added from stock solutions. For the recording of tryptophan emission fluorescence spectra (300–550 nm) the excitation wavelength was set to 295 nm to minimize the contribution of tyrosine. Backgrounds readings were subtracted and the wavelength and fluorescence maximum values recorded. Corrections were made to compensate for protein dilution. The data analysis was carried out with the Spectra Calc program (Galactica Corp). The fractional saturation binding by fructose-6-P was determined from the intensity variation with free ligand concentration by calculating the quantity $(F^0–F)/(F^0–F^\infty)$, where $F^0$ represents the emission intensity in the absence of ligand, $F^\infty$ is the emission intensity at saturating concentration of ligand, and $F$ is the intensity after addition of a given ligand concentration.

*Dynamic light-scattering measurements*

Studies were carried out at 20 ± 0.1 °C using a DynaPro-MS800 dynamic light-scattering instrument from Protein Solutions, Inc. Samples containing purified D256N Pfk-2 (1 mg/ml) in 25 mM Tris–HCl buffer, pH 7.5, 5 mM MgCl2, 1 mM DTT, and the indicated concentrations of MgATP, were centrifuged for 10 min at 14,000 rpm in an Eppendorf microfuge to remove particulate matter. In dynamic light-scattering experiments, the hydrodynamic radius of the particle is calculated via the Stokes–Einstein equation from the diffusion coefficient, which is obtained from the measured autocorrelation function [31], using the DYNAMICS Software supplied with the instrument.

*Size-exclusion chromatography*

Size-exclusion chromatography was performed using a Water Breeze HPLC system equipped with a Bio-Rad exclusion column (Bio-Sil SEC 250). Calibration was performed by using the proteins provided by the manufacturer of the column. Protein elution was followed at 280 nm.

## Results

*Structure-based phylogeny of the ribokinase family*

All the ribokinase family members with known structure, 32 proteins (Table 1), were obtained from the PDB and used for phylogenetic analysis. Although they are annotated as kinases in the corresponding PDB file, their phosphoryl acceptor was either unknown or not unambiguously defined for 13 of them. In 14 cases, the cognate substrate (or product) was found at the phosphoryl acceptor site in the structure model. These structures were superposed in order to obtain a MSA based on structural information. This MSA was subsequently used for phylogenetic inference by

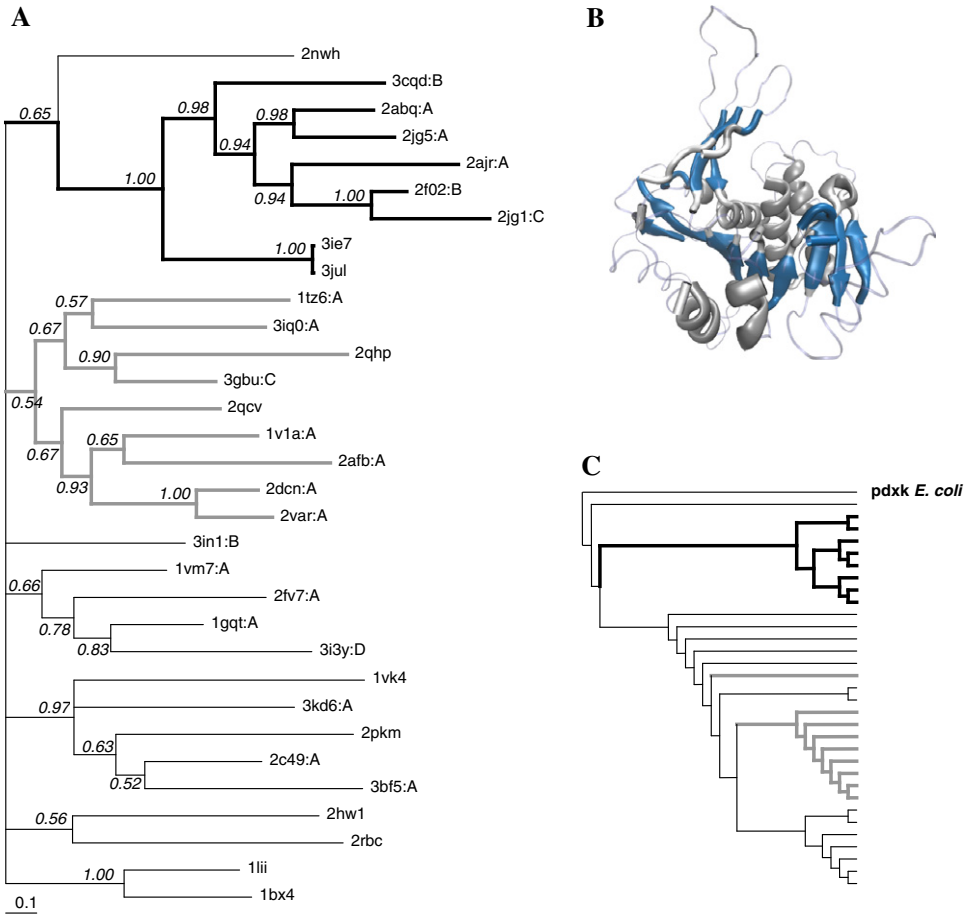


**Fig. 1.** Phylogeny of ribokinase family members with known structure. (A) Dendrogram constructed by bayesian phylogenetic inference of a sequence alignment derived from structural superposition. Taxa are labeled with the pdb code of the protein (when there is more than one, the chain under analysis is indicated after colon). Numbers at nodes indicate posterior probabilities. The bar at the bottom indicates the distance corresponding to 0.1 substitutions per site. Bold branches are used for PfkB subfamily members. Gray branches are used to highlight the close relationship between AIRs/fructose kinases and deoxygluconate kinases. (B) Structural representation of the regions remaining after removal of all gap-containing positions from the structure-based sequence alignment. Strands (blue) and helices (gray) are shown as thick ribbons. Thin ribbons represent the entire polypeptide chain of Pfk-2. The resulting 188 positions correspond to the core of the ribokinase-like fold. (C) UPGMA tree of QH index (metrics of structural similarity) for the taxa shown in (A) and pyridoxal kinase from *E. coli* (2DDW, chain A) used as outgroup. (For interpretation of the references to color in this figure legend, the reader is referred to the web version of this paper.)

the Bayesian method and the resulting phylogenetic dendrogram is shown in Fig. 1A.

The phosphosugar kinases (thick lines) form a single clade, the PfkB subfamily, with a posterior probability of 1. The phosphosugar kinases from *Listeria* branch off first from the clade. The specificity towards fructose-6-P seems to have appeared previous to the differentiation between fructose-1-P and tagatose-6-P kinase activities. The carbohydrate kinase from *Agrobacterium*, 2nwh, with unknown substrate specificity, is related to the PfkB subfamily closer than other taxa, with a posterior probability of 0.65.

The keto-deoxygluconate kinase clade is supported by a posterior probability value of 0.67 and segregate together with AIRs kinase from *Salmonella*, fructokinase from *Bacteroides* and two sugar kinases annotated as "E.C. 2.7.1.-", with a posterior probability of 0.54. We can distinguish the ribokinase and eukaryotic adenosine kinase subfamilies as separated clades. Interestingly, the nucleoside kinases from *Chlorobium* and *Methanocaldococcus* form a monophyletic group with adenosine kinase from *Mycobacterium* (together with two putative carbohydrate kinases), supported by a good posterior probability. Only 3in1, the uncharacterized sugar kinase YDJH from *E. coli*, was not associated to any clade.

In order to determine the most primitive branching in the evolutionary pathway of ribokinase family we use the structure of pyridoxal kinase (PdxK) from *E. coli* [32] as outgroup under the assumption that it diverged from the last common ancestor of the superfamily previous to the diversification of ribokinase family [13]. An UPGMA tree was built by Multiseq in VMD by using the structural measure QH, algorithm that calculates the structural similarity of each residue in a set of aligned structures and accounts for the presence of insertions in the structure [23]. In this tree (Fig. 1C), the PfkB subfamily and 2nwh locates closer to PdxK than other taxa, indicating that they are the most primitive group to emerge within the ribokinase family. Except for a missing member, the AIRs/fructokinases are also associated to keto-deoxygluconate kinases closer than to other taxa in this tree (gray lines). Thus, we propose a basal character of PfkB subfamily in the evolution of the ribokinase family and a close relationship between AIRs/fructose and ketodeoxygluconate subfamilies.

### *Conserved residues in the active site of PfKB subfamily members*

The structure of tagatose-6-P kinase from *S. aureus* illustrates the interactions pattern that must be established when a phosphosugar binds. Fig. 2A shows a structural superposition of the phosphoryl acceptor site of tagatose-6-P kinase from *S. aureus* and Pfk-2. The residues that establish hydrogen bonds with the oxygen atoms of the phosphate moiety are shown for tagatose-6-P kinase together with the equivalent ones in Pfk-2. These residues are: an

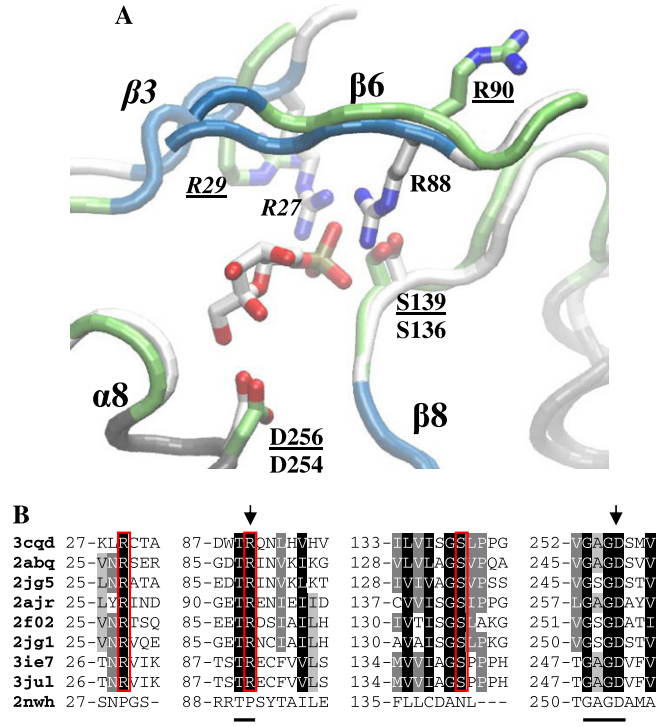


**Fig. 2.** Conserved residues in the active site of PfkB subfamily members. (A) Structural superposition of phosphotagatose kinase from *S. aureus* with fructose-6-P bound and Pfk-2 from *E. coli*, showing conserved residues involved in interactions with the phosphate and hydroxymethyl moieties of the substrate. Underlined residues correspond to Pfk-2. Residues and secondary structural elements from the adjacent subunit of the dimer are indicated in italics. (B) Structure-based multiple sequence alignment of the PfkB subfamily enzymes, illustrating the conservation of the regions around the residues shown in (A). Arrows indicate the position of residues from the TR and GXGD motifs (indicated by lines) that were selected for mutation in Pfk-2.

arginine coming from the adjacent subunit in the dimer (29 in Pfk-2 and 27 in tagatose-6-P kinase); another arginine located in the loop that connects β5 in the major domain to β6 in the minor domain (90 in Pfk-2 and 88 in tagatose-6-P kinase); and a serine previously identified by Miallau et al. [4] (139 in Pfk-2 and 136 in tagatose-6-P kinase), located in the major domain in the loop following β8. These three residues are conserved among all the PfkB subfamily members (Fig. 2B) and form a structural signature probably involved in the binding of the phosphate moiety of the sugar. We regard them as the "RRS sugar-phosphate binding triad" that specifically identifies PfkB subfamily members among other members of the ribokinase family. For example, the triad is absent from the close relative 2nwh, the carbohydrate kinase from *Agrobacterium* (Fig 2B).

The conserved R from the adjacent subunit and S, although being a specific feature of the PfkB subfamily that could not be found in other members of the ribokinase family, are located in variable regions that were taken off in the process of MSA generation because of the lack of corresponding positions in the rest of the structures. However, the region in which the RT-sequence motif is present has structural counterparts in the other members of the ribokinase family, but (of course) only phosphosugar kinases present an arginine in this position.

On the other hand, the hydroxymethyl moiety in the phosphosugar is oriented towards the N-terminal turn of helix 8, which contains the GXGD motif (Fig. 2B), highly conserved among the members of the ribokinase family [22]. The carboxylate of this aspartic residue is at hydrogen-bond distance of the hydroxyl group that accepts the γ-phosphate in tagatose-6-P kinase. In Pfk-2 this residue corresponds to D256.

Thus, on one hand we predict, for the sugar phosphate kinases, that the interactions of R, from the TR sequence motif, with the phosphoryl moiety of the sugar substrate, will mainly affect the affinity for the sugar substrate. On the other hand, the interaction of D from GXGD motif with the hydroxymethyl moiety of the substrate will affect the catalytic efficiency. In order to evaluate whether such a functional segregation indeed occurs, R90 and D256 were examined with regard to their function in substrate binding and catalysis in Pfk-2 from *E. coli*. We take this enzyme as a model system since it is the most well characterized member of the PfkB subfamily, biochemically and structurally speaking.

### *The arginine residue from the TR motif and its effect on substrate binding in Pfk-2*

In order to evaluate the importance of the charge present in R90 on the interaction with the phosphorylated substrate, fructose-6-P, we changed this residue to glutamine (R90Q) by site-directed mutagenesis. Although smaller than R, Q has a longer polar side chain. Kinetic experiments and intrinsic fluorescence measurements indicate that in the R90Q mutant the interaction with the fructose-6-P substrate was highly impaired. The kinetic behavior of the R90Q mutant for the sugar substrate is hyperbolic (Fig. 3A), but the $K_M$ value is increased approximately 200-fold rel-

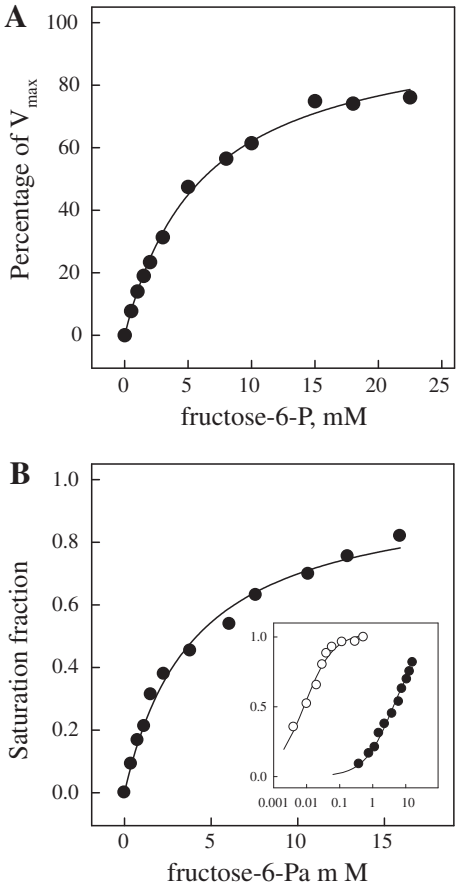


**Fig. 3.** Effect of the R90Q mutation of Pfk-2 on kinetics and binding of fructose-6-P. (A) Percentage of apparent $V_{max}$ obtained from initial velocity measurements of the R90Q enzyme as a function of the fructose-6-P concentration. For $k_{cat}$ and $K_M$ values see Table 2. (B) Binding of fructose-6-P to the R90Q enzyme determined by intrinsic fluorescence measurements. Inset shows the binding curves for fructose-6-P for wild type Pfk-2 (○) and the R90Q mutant (●) in logarithmic scale, using the same units of axes as graph (B). The excitation wavelength was 295 nm; the excitation and emission slits were both 5 nm.

ative to the wild type enzyme (Table 2). Titration of the R90Q mutant with fructose-6-P produces a quenching of the intrinsic fluorescence of about 20% near to saturation conditions. The dissociation constant determined by intrinsic fluorescence measurements for fructose-6-P binding was 600-fold higher in R90Q than in the wild type enzyme. Other kinetic parameters such as the $K_M$ value for MgATP or $k_{cat}$ were slightly lower compared to wild type Pfk-2 (Table 2). Regarding the possible effect over the allosteric properties of the R90Q mutant, the inhibition produced by the allosteric effector is still observed when using near-to-$K_M$ concentrations of fructose-6-P (5 mM), as observed in Fig. 4. Upon increasing the fructose-6-P substrate concentration to 18 mM the inhibitory effect appears to be partially relieved as it is also observed for the wild type enzyme. It was difficult to achieve saturating concentrations of fructose-6-P in order to provide conditions for total relief of the MgATP inhibition, given the high value of the determined apparent $K_M$. However, MgATP-induced tetramerization of R90Q occurs (Fig. 4, inset) in a similar fashion to the wild type enzyme, as previously reported [33].

*The aspartic residue from the GXGD motif and its effect on catalysis in Pfk2*

To evaluate the role of D256 in catalysis and substrate binding in Pfk-2 we performed site-directed mutagenesis of this residue to asparagine. With this change the size of the residue is maintained while the charge is ablated but kept polar. Circular dichroism spectra from the mutant and wild type enzymes were found to be virtually superimposable (data not shown), indicating that the mutation did not produce major changes in the secondary structure of the mutant enzyme. In Table 2, the kinetic properties of the D256N mutant are summarized. Replacement of the aspartic residue by asparagine produces a striking decrease of 15,000-fold in the catalytic constant, while the $K_M$ values for fructose-6-P or MgATP show no significant variation as compared to the wild type enzyme. These results support the idea that D256 participates specifically in catalysis, being less important in other processes such as substrate binding or allosteric regulation by MgATP. Indeed, inhibition of the enzyme activity by MgATP occurred at non-saturating concentrations of fructose-6-P (Fig. 5). The effect of increasing these concentrations on the inhibition behavior was very similar to that observed for the wild type enzyme [29]. The other consequence of the allosteric binding of MgATP, the oligomerization of the native dimers into tetramers, was asserted in the mutant enzyme by using dynamic light-scattering measurements. The D256N enzyme changed its hydrodynamic radius from 3.76 to 4.34 Å with a half-saturation concentration of 55 μM (Fig. 5B). A comparable change was previously determined for wild type Pfk-2 [33]. These results support our hypothesis that the interaction of D256 with the hydroxymethyl moiety of the substrate mainly determines the catalytic rate of the phosphoryl transfer reaction.

**Table 2**
Kinetic and ligand binding parameters of wild type Pfk-2 and R90Q and D256N mutants.

| | Wild type | R90Q | D256 N |
|---|---|---|---|
| $k_{cat}$, $s^{-1}$ | 53 ± 2.4 | 39 ± 5 | 0.0035 |
| $K_M$ MgATP, μM | 22 ± 4.9 | 8 ± 1.5 | 73 |
| $K_M$ fru-6-P, μM | 28 ± 2.3 | 6000 ± 500 | 30 |
| [a]$K_d$ fru-6-P, μM | 6 (30%) | 4000 (20%) | n.d. |

[a] $K_d$ value was obtained from intrinsic fluorescence measurements. The % of increase (wild type) or quenching (R90Q mutant) of fluorescence was indicated in parenthesis.
n.d. not determined.

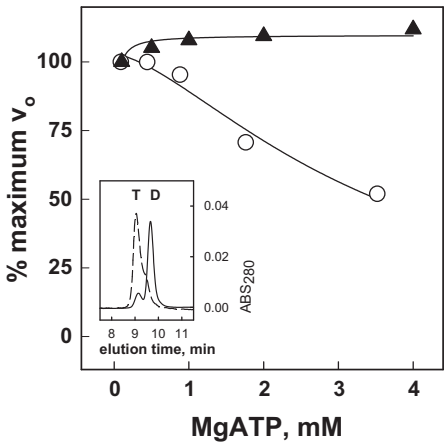


**Fig. 4.** Inhibition by MgATP in the R90Q mutant. Increment of MgATP concentration was done keeping free $Mg^{+2}$ concentration at 2 mM. For each fructose-6-P concentration the activity observed at 1 mM MgATP was taken as the 100%. Inset. MgATP-induced tetramerization. Size-exclusion chromatography was performed in the absence (solid line) and presence (dashed line) of 0.5 mM MgATP. T and D indicate the elution volume of tetramer and dimer, respectively.

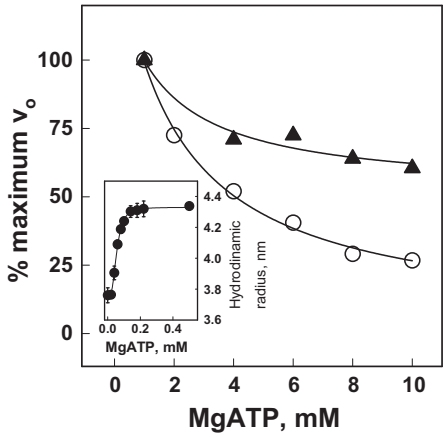


**Fig. 5.** Inhibition and tetramerization by MgATP in the D256 N mutant. (A) The effect of MgATP on the enzyme activity of D256N mutant was measured at 0.1 mM (●) and 1 mM (○) fructose-6-P. Inset. Dynamic light-scattering measurements of the mutant enzyme at different MgATP concentrations. Data correspond to the average of four determinations with its standard deviation. Fitting to a sigmoidal function gave a $K_{0.5}$ of 54 μM and a $n_h$ of 3.1.

## Discussion

Evolutionary trees of the ribokinase family have been previously proposed using substitution matrix-based alignments [7,8]. However, conventional MSA methods are less effective in determining equivalent positions when comparing proteins with low levels of percentage of sequence identity, as is the case for ribokinase family members. Then, we restricted our analysis to members with known structure to obtain a sequence alignment by structural superposition. In agreement with previous results, the phosphosugar kinases were observed to form a monophyletic group. We denominate this clade the PfkB subfamily. Furthermore, we propose that PfkBs descent from a common ancestor that emerged early in the evolutionary history of the ribokinase family. In their phylogenetic tree, Park and Gupta (2008) [8] identified groups corresponding to fructokinases, ribokinases, bifunctional *D*-hepta-D-heptose-7-phosphate kinases, adenosine kinases, tagatose-6-P kinases, phosphofructokinases and ketohexokinases. Here we suggest a close kinship between AIR-skinase, fructokinases and ketodeoxy gluconate kinases. Also, we

found a possible monophyletic group that congregates nucleoside kinases from *Chlorobium* and *Methanocaldococcus* and adenosine kinase from *Mycobacterium*.

As described for tagatose-6-P kinase [4], the phosphate moiety of the substrate establishes interactions with conserved residues specific for the phosphosugar kinase group:two arginine and one serine residues (Fig. 2B). On the other hand, interactions of the hydroxyl moiety with an aspartic residue, conserved at the family level, play an important role in catalysis, according to the proposed model for the catalytic mechanism of the ribokinase family [22]. In 1-phosphofructokinase from *Bacillus allodurans* (PDB id. 2abq) serine 134 is hydrogen-bonded to a phosphate ligand present at the sugar site (not shown) slightly displaced from the location observed for the phosphate moiety of tagatose-6-P in tagatose-6-P kinases. Thus, the identification of potential specificity towards phosphosugars among the members of the ribokinase family could be inferred from sequences matching the motifs shown in Fig. 2B. For example, according to this, the 2nwh could not be classified as a phosphosugar kinase, in spite of its close relationship, as shown in Fig. 1.

Our site-directed mutagenesis results demonstrated that R90 of the TR sequence motif in Pfk-2 indeed participates in the interaction with the phosphorylated sugar substrate, most probably by stabilizing the negative charge of the 6-phosphate group as observed in phosphotagatose kinase (Fig. 2A). In the crystal structure of Pfk-2 in complex with substrate and allosteric ATPs, the R90 residue interacts with W88. Consequently, the different effect of fructose-6-P on the the intrinsic fluorescence of R90Q and wild type is not unexpected. (Table 2). Other features such as MgATP-induced inhibition and tetramerization are still observed, which support that the role of this residue is restricted to the interaction with the sugar-phosphate at the active site. From the conserved residues in Fig. 2B, only those forming the structural signature RRS triad are involved in the binding of the phosphate group of the sugar-phosphate, and are specifically conserved among the PfkB subfamily members. The Thr residue in the TR sequence motif is conserved at the family level, being occasionally substituted by Ser. In Pfk-2, the hydroxyl group of Thr89 establishes a hydrogen bond with NH from Gly69. This interaction seems to be important to restrain the orientation of the polypeptide chain in a region that forms part of the hinge between major and minor domains. Due to the conservation of these residues, Thr and Gly (not shown), this would be a common feature of the ribokinase family tertiary structure. In Pfk-2, the side chain of R29 and R90 lay outside the active site suggesting a conformational change that reorients them taking place upon fructose-6-P binding. It is well known that arginine residues are involved in binding and stabilization of negatively charged groups of substrates or coenzymes [34].

Regarding the conserved aspartic acid our site-directed mutagenesis results indicate that the absence of the negative charge from D in the GXGD motif profoundly and almost exclusively affects the turnover number of Pfk-2. Regulatory properties such as inhibition and tetramerization remain mostly unaffected (Fig. 5). In this way, our results support that the mechanism for the phosphoryl transfer, in which aspartic acid acts as a general base to abstract the proton from the hydroxymethyl moiety, is conserved also among the phosphosugar kinases of the ribokinase family. In *E. coli* ribokinase, the interactions of the enzyme with ribose suggest that D256 acts as the base that abstract a proton from the O5′-hydroxyl group of sugar [9]. In the structure of human adenosine kinase, D300 bridges the O5́atom of the adenosine substrate, as well as a $Mg^{2+}$ ion (proposed to be important for phosphoryl transfer) [10]. In adenosine kinase from *T. gondii* the corresponding residue D318 is well positioned for proton abstraction of the adenosine 5′hydroxyl group [12]. In adenosine kinase from *L. donovani* mutation of D299 to alanine leads to a complete loss of activity [35]. The catalytic role of conserved aspartate residue acting as a general base is well established also at the superfamily level. The only exceptions are THZ kinase and HMPP kinase, which have cysteine as a catalytic base for the activation of the phosphate acceptor in a nucleophilic attack [36,37]. In ADP-dependent glucokinases this aspartate residue is also conserved, being D440 in the enzyme from *Pyrococcus* [38] and D451 in the enzyme from *Thermococcus* [39].

Segregation of binding and catalytic interactions is observed for the mutants tested. Interestingly, in the analogous isozyme Pfk-1 (convergent in function but not related by a common ancestor to Pfk-2) R162 and R243 interact with the 6-phosphate moiety of fructose-6-P [40]. Substitution of these residues to serine results in enzymes with deceased fructose-6-P binding ability and reduced cooperativity but little change in catalytic ability. Conversely, R72 participates in the differential stabilization of the transition state of this enzyme. The essential function of an aspartate group in the catalysis of phosphoryl transfer has been demonstrated for Pfk-1 [41]. Mutation of this residue to serine decreases the catalytic activity of the enzyme by 15,000–18,000 fold compared to the wild type, highlighting striking resemblances in substrate binding and catalytic mechanisms of otherwise unrelated phosphofructokinases from *E. coli*.

## Conclusions

We used a non-redundant dataset of ribokinase family members obtained from the Protein Data Bank to perform phylogenetic analysis by the Bayesian method and to dissect between globally conserved positions and positions common to the phosphosugar kinases subset. In this way, we identified two sequence conserved motifs predicted to be involved in interactions with the phosphosugar substrate: the TR motif, not described previously, present in phosphosugar kinases but not in other members of the ribokinase family, and the globally conserved motif GXGD. Using Pfk-2 as a study model, site-directed mutagenesis of residues present in these motifs (R90 and D256) was performed. Analysis of kinetic and binding properties of these mutants indicates that R90 participates in binding of the phosphorylated substrate and that D256 is involved in the phosphoryl transfer mechanism in Pfk-2.

## Acknowledgments

This work was supported by grants from Fondo Nacional de Desarrollo Científico y Tecnológico (Fondecyt 1040892 and 1070111). We thank P. Villalobos and P. Ayala for their assistance in the preparation of graphical material.

## References

[1] R. Cabrera, A.L. Ambrosio, R.C. Garratt, V.Guixé,J. Babul, J. Mol. Biol. 383 (2008) 588–602.
[2] V. Guixé, J. Babul, Arch. Biochem. Biophys. 264 (1988) 519–524.
[3] J.C. Torres, V. Guixé, J. Babul, Biochem. J. 327 (1997) 675–684.
[4] L. Miallau, W.N. Hunter, S.M. McSweeney, G.A. Leonard, J. Biol. Chem. 282 (2007) 19948–19957.
[5] L.M. Orchard, H.L. Kornberg, Proc. Biol. Sci. 242 (1990) 87–90.
[6] L.F. Wu, A. Reizer, J. Reizer, B. Cai, J.M. Tomich, M.H. Saier Jr, J. Bacteriol. 173 (1991) 3117–3127.
[7] P. Bork, C. Sander, A. Valencia, Protein Sci. 2 (1993) 31–40.
[8] J. Park, R.S. Gupta, Cell Mol. Life Sci. 65 (2008) 2875–2896.
[9] J.A. Sigrell, A.D. Cameron, T.A. Jones, S.L. Mowbray, Structure 6 (1998) 183–193.
[10] I.I. Mathews, M.D. Erion, S.E. Ealick, Biochemistry 37 (1998) 15607–15620.
[11] W.J. Cook, L.J. DeLucas, D. Chattopadhyay, Protein Sci. 9 (2000) 704–712.
[12] M.A. Schumacher, D.M. Scott, I.I. Mathews, S.E. Ealick, D.S. Roos, B. Ullman, R.G. Brennan, J. Mol. Biol. 296 (2000) 549–567.
[13] Y. Zhang, M. Dougherty, D.M. Downs, S.E. Ealick, Structure 12 (2004) 1809–1821.

[14] N. Ohshima, E. Inagaki, K. Yasuike, K. Takio, T.H. Tahirov, J. Mol. Biol. 340 (2004) 477–489.
[15] L. Arnfors, T. Hansen, P. Schonheit, R. Ladenstein, W. Meining, Acta Crystallogr. D. Biol. Crystallogr. 62 (2006) 1085–1097.
[16] M.C. Reddy, S.K. Palaninathan, N.D. Shetty, J.L. Owen, M.D. Watson, J.C. Sacchettini, J. Biol Chem. 282 (2007) 27334–27342.
[17] I.I. Mathews, D. McMullan, M.D. Miller, J.M. Canaves, M.A. Elsliger, R. Floyd, S.K. Grzechnik, L. Jaroszewski, H.E. Klock, E. Koesema, J.S. Kovarik, A. Kreusch, P. Kuhn, T.M. McPhillips, A.T. Morse, K. Quijano, C.L. Rife, R. Schwarzenbacher, G. Spraggon, R.C. Stevens, Proteins 70 (2008) 603–608.
[18] J.A. Potter, M. Kerou, H.J. Lamble, S.D. Bull, D.W. Hough, M.J. Danson, G.L. Taylor, Acta Crystallogr. D. Biol. Crystallogr. 64 (2008) 1283–1287.
[19] C.H. Trinh, A. Asipu, D.T. Bonthron, S.E. Phillips, Acta Crystallogr. D. Biol. Crystallogr. 65 (2009) 201–211.
[20] A.G. Murzin, S.E. Brenner, T. Hubbard, C. Chothia, J. Mol. Biol. 247 (1995) 536–540.
[21] A.L. Cuff, I. Sillitoe, T. Lewis, O.C. Redfern, R. Garratt, J. Thornton, C.A. Orengo, Nucleic Acids Res. 37 (2009) D310–314.
[22] V. Guixé, F. Merino, IUBMB Life 61 (2009) 753–761.
[23] E. Roberts, J. Eargle, D. Wright, Z. Luthey-Schulten, BMC Bioinformatics 7 (2006) 382.
[24] W. Humphrey, A. Dalke, K. Schulten, J. Mol. Graph. 14 (1996) 33–38, 27–28.
[25] Available from: http://www.nrbsc.org/gfx/genedoc/ebinet.htm.
[26] F. Ronquist, J.P. Huelsenbeck, Bioinformatics 19 (2003) 1572–1574.
[27] S. Tabor and C. C. Richardson, Proc. Natl. Acad. Sci. (USA) 82 (1985) 1074–1078.
[28] J. Babul, J. Biol. Chem. 253 (1978) 4350–4355.
[29] V. Guixé, J. Babul, J. Biol. Chem. 260 (1985) 11001–11005.
[30] V. Guixé, P.H. Rodriguez, J. Babul, Biochemistry 37 (1998) 13269–13275.
[31] Dynamic Light Scattering: Applications of Photon Correlation Spectroscopy, R. Pecora (Ed.), Plenum, New York, 1985.
[32] M.K. Safo, F.N. Musayev, J. Bacteriol. 188 (2006) 4542–4552.
[33] R. Cabrera, V. Guixé, J. Alfaro, P.H. Rodriguez, J. Babul, Arch. Biochem. Biophys. 406 (2002) 289–295.
[34] J.F. Riordan, K.D. McElvany, C.L. Borders Jr., Science 195 (1977) 884–886.
[35] R. Datta, I. Das, B. Sen, A. Chakraborty, S. Adak, C. Mandal, A.K. Datta, Biochem. J. 387 (2005) 591–600.
[36] N. Campobasso, I.I. Mathews, T.P. Begley, S.E. Ealick, Biochemistry 39 (2000) 7868–7877.
[37] G. Cheng, E.M. Bennett, T.P. Begley, S.E. Ealick, Structure 10 (2002) 225–235.
[38] S. Ito, S. Fushinobu, J.J. Jeong, I. Yoshioka, S. Koga, H. Shoun, T. Wakagi, J. Mol. Biol. 331 (2003) 871–883.
[39] S. Ito, S. Fushinobu, I. Yoshioka, S. Koga, H. Matsuzawa, T. Wakagi, Structure 9 (2001) 205–214.
[40] S.A. Berger, P.R. Evans, Nature 343 (1990) 575–576.
[41] H.W. Hellinga, P.R. Evans, Nature 327 (1987) 437–439.